

# Neutron scattering investigation of proposed Kosterlitz-Thouless transitions in the triangular-lattice Ising antiferromagnet $\text{TmMgGaO}_4$

Zhiling Dun,<sup>1</sup> Marcus Daum,<sup>1</sup> Raju Baral,<sup>2</sup> Henry E. Fischer,<sup>3</sup> Huibo Cao,<sup>4</sup> Yaohua Liu,<sup>4</sup> Matthew B. Stone,<sup>4</sup> Jose A. Rodriguez-Rivera,<sup>5,6</sup> Eun Sang Choi,<sup>7</sup> Qing Huang,<sup>8</sup> Haidong Zhou,<sup>8</sup> Martin Mourigal,<sup>1</sup> and Benjamin Frandsen<sup>2</sup>

<sup>1</sup>*School of Physics, Georgia Institute of Technology, Atlanta, GA 30332, USA*

<sup>2</sup>*Department of Physics and Astronomy, Brigham Young University, Provo, UT 84602, USA*

<sup>3</sup>*Institut Laue-Langevin, BP 156, 38042 Grenoble Cedex 9, France*

<sup>4</sup>*Neutron Scattering Division, Oak Ridge National Laboratory, Oak Ridge, TN 37831, USA*

<sup>5</sup>*Department of Materials Sciences, University of Maryland, College Park, Maryland 20742, USA*

<sup>6</sup>*NIST Center for Neutron Research, Gaithersburg, MD 20899, USA*

<sup>7</sup>*National High Magnetic Field Laboratory, Florida State University, Tallahassee, FL, 32306, USA*

<sup>8</sup>*Department of Physics and Astronomy, University of Tennessee, Knoxville, TN 37996, USA*

(Dated: December 3, 2023)

The transverse-field Ising model on the triangular lattice is expected to host an intermediate finite-temperature Kosterlitz-Thouless (KT) phase through a mapping of the spins on each triangular unit to a complex order parameter.  $\text{TmMgGaO}_4$  is a candidate material to realize such physics due to the non-Kramers nature of  $\text{Tm}^{3+}$  ion and the resulting two-singlet single-ion ground state. Using inelastic neutron scattering, we confirm this picture by determining the leading parameters of the low-energy effective Hamiltonian of  $\text{TmMgGaO}_4$ . Subsequently, we track the predicted KT phase and related transitions by inspecting the field and temperature dependence of the ac susceptibility. We further probe the spin correlations in both reciprocal space and real space via single crystal neutron diffraction and magnetic total scattering techniques, respectively. Magnetic pair distribution function analysis provides evidence for the formation of vortex-antivortex pairs that characterize the proposed KT phase around 5 K. Although structural disorder influences the field-induced behavior of  $\text{TmMgGaO}_4$ , the magnetism in zero field appears relatively free from these effects. These results position  $\text{TmMgGaO}_4$  as a strong candidate for a solid-state realization of KT physics in a dense spin system.

Interacting Ising spins in a transverse magnetic field display important quantum many-body effects [1], including quantum phase transitions [2, 3] and order by disorder [4]. Frustrated magnets comprised of non-Kramers ions in a low-symmetry crystal field, such as the pyrochlore materials  $\text{Pr}_2\text{Zr}(\text{Hf})_2\text{O}_7$  [5–7] and the kagome magnet  $\text{Ho}_3\text{Mg}_2\text{Sb}_3\text{O}_{14}$  [8, 9], host a two-singlet ground-state that maps onto an intrinsic transverse field acting on Ising spins [10], which can promote quantum fluctuations [11] and entanglement [12]. In models where such magnetic ions decorate a triangular lattice, the transverse field induces a three-sublattice (3SL) order for antiferromagnetically coupled Ising spins through a quantum order by disorder phenomenon [4, 13]. This can be re-cast as a two-dimensional  $XY$  model with a  $Z_6$  clock term [14, 15], for which two finite-temperature Kosterlitz-Thouless (KT) transitions are expected to border an intermediate phase with power-law spin correlations [16]. These deep theoretical insights offer the enticing opportunity to realize the topological vortex-pair binding and unbinding transitions proposed by Kosterlitz and Thouless in 1973 [17] in a dense spin system.

The recently synthesized rare-earth antiferromagnet  $\text{TmMgGaO}_4$  [18] has been proposed to realize the transverse-field Ising model on the triangular-lattice [19, 20]. This material derives from the intensely studied quantum spin-liquid candidate  $\text{YbMgGaO}_4$  [21–23], where  $\text{Yb}^{3+}$ , a Kramers ion, is replaced by  $\text{Tm}^{3+}$ , a non-Kramers ion. In  $\text{TmMgGaO}_4$ , the crystal electric field forces the dipolar magnetic moments to point out of the triangular plane (crystallographic  $c$ -axis) while the in-plane components transform as magnetic multipoles [19, 24]. The two-singlet ground-

state, and thus the transverse field, appears accidentally in  $\text{TmMgGaO}_4$  from the octahedral environment of oxygen ligands [25]. Previous neutron scattering studies [19, 20] uncovered the predicted 3SL order below  $T = 1$  K, although no corresponding anomalies were observed in specific heat or magnetic susceptibility measurements. Theoretical studies suggest that the 3SL order reflects the departure from the proposed KT phase at low-temperature ( $T \equiv T_l$ ) [24, 26] and that another KT transition exists at a higher temperature ( $T_h \approx 4$  K) [26], corresponding to the unbinding of vortex-antivortex (V-AV) pairs. These vortices emerge via a mapping from the  $S^z$  components of the  $\text{Tm}^{3+}$  spins to a complex order parameter,  $\psi = |\psi|e^{i\theta} = S_A^z + e^{i2\pi/3}S_B^z + e^{i4\pi/3}S_C^z$ , where A, B and C are the sublattice indices of the 3SL order [26, 27]. So far, no experimental probes have detected the transition at  $T_h$ . Moreover, in light of the intrinsic Mg-Ga structural disorder that strongly affects the low-temperature magnetism of the iso-structural compound  $\text{YbMgGaO}_4$  [20, 23, 28–30], it is unclear whether or not KT physics survives in  $\text{TmMgGaO}_4$ .

In this Letter, we search for the proposed KT transitions in  $\text{TmMgGaO}_4$  using ac magnetometry to inspect scaling predictions [15, 26, 31] and neutron scattering measurements in the field-polarized and paramagnetic phases to ascertain the material’s Hamiltonian. We track the temperature-dependent spin correlations in both reciprocal and real space, the latter using magnetic pair distribution function analysis [32, 33]. Our analysis evidences two possible transitions at  $T_h \approx 5$  K and  $T_l \approx 0.9$  K with a continuous increase in correlation length over almost two decades in temperature. In our experiments,  $T_l$  reflects the gradual condensation of two-dimensional mag-

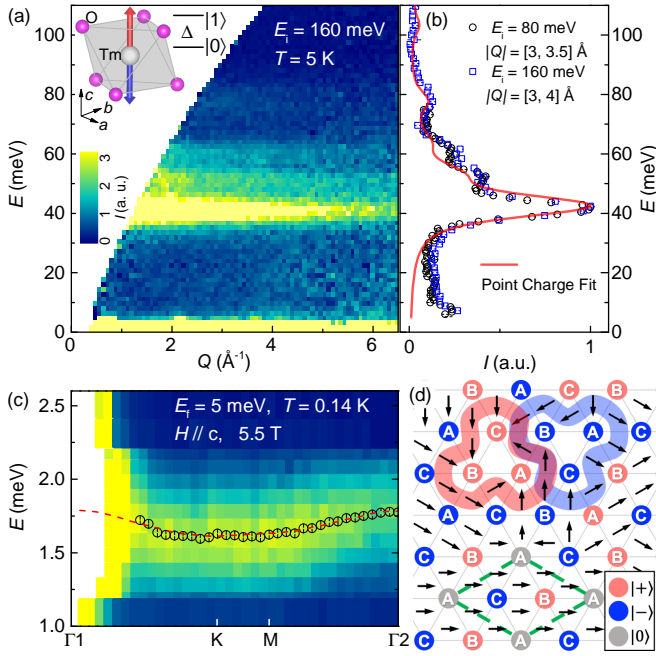


FIG. 1. (a) Inelastic neutron scattering intensity  $I(Q, E)$  from broad-band measurements of  $\text{TmMgGaO}_4$  at  $T = 5$  K and  $E_i = 160$  meV. Inset: oxygen ligands (pink spheres) around each  $\text{Tm}^{3+}$  ion (grey sphere) and the resulting spin anisotropy (arrows). (b) Scattering intensity at low momentum-transfer  $Q$ . Best fit using an effective point-charge model (red line) [25] (see SI). (c) Low-energy spin excitations at  $T = 50$  mK under an external magnetic field of  $\mu_0 H = 5.5$  T applied along the  $c$ -axis. Solid circles represent the peak centers from Gaussian fits to constant- $Q$  cuts, and the dashed red line represents the best fit using Eq. 1 based on linear spin wave theory. (d) Bound vortex-antivortex (V-AV) pair (upper half) and the 3SL order (lower half), where the green dashed lines show the magnetic unit cell. Red, blue, and grey circles represent up ( $|+\rangle$ ), down ( $|-\rangle$ ), and nonmagnetic ( $|0\rangle$ ) spins, respectively. Black arrows represent  $\psi$ . The red (blue) shaded region illustrates a vortex (antivortex) in the spatial arrangement of  $\psi$ , characterized by an emergent topological charge equal to the winding number of  $\psi$  around the path [26].

netic scattering at the  $K$ -point of the triangular Brillouin zone (corresponding to the 3SL order), although the correlation length remains finite in the plane down to at least 280 mK. Real-space analysis at higher temperature demonstrates that the spin correlations around  $T_h$  deviate from the 3SL short-range order in a manner consistent with the formation of V-AV pairs. Our work provides solid – albeit indirect – evidence for KT physics in  $\text{TmMgGaO}_4$  and reveals that the significant structural disorder in this compound does not appear to profoundly impact the zero-field physics.

We start with the validation of the effective spin-1/2 Hamiltonian for  $\text{TmMgGaO}_4$ . Broad-band inelastic neutron scattering experiments using the SEQUOIA spectrometer [34] at Oak Ridge National Laboratory (ORNL) [see Supplementary Information (SI) for details] reveal crystal electric-field (CEF) excitations for an energy transfer  $E$  between 30 and 90 meV,

with the expected decrease in scattering intensity  $I(Q, E)$  at large momentum transfer  $Q$  [Fig. 1(a)]. Four excitations occur at 41.9(1), 52.6(1), 61.4(2), and 78.7(2) meV, respectively [black circles, Fig. 1(b)], with the 41.9 meV mode corresponding to the first excited CEF level above the two-singlet ground state (see SI). The  $\Delta E \approx 7.5$ –10 meV width of the CEF peaks does not depend on the incident neutron energy, and is much broader than the instrumental resolution, suggesting it is an intrinsic effect reminiscent of  $\text{YbMgGaO}_4$  [23, 28]. We use the effective point charge model outlined in Ref. [25] to fit the excitation spectrum using only three parameters [Fig. 1(b)]. The best fit captures the energy of the four CEF excitations successfully, except for a mismatch in intensity. An alternative fit using the Steven's operators method can be found in SI. This analysis yields a CEF ground-state comprising two-singlets,  $|0\rangle \approx 1/\sqrt{2}(|+\rangle + |-\rangle)$  and  $|1\rangle \approx 1/\sqrt{2}(|+\rangle - |-\rangle)$ , which are symmetric and antisymmetric combinations of states from the non-Kramers doublet:  $|\pm\rangle = 0.939|\pm 6\rangle + 0.314|\pm 3\rangle + 0.111|0\rangle$  in the  $|J = 6, J_z\rangle$  basis, with an energy separation of  $\Delta = 0.24$  meV. This validates the mapping to an effective transverse-field Ising model [9, 19] by which the CEF Hamiltonian reads  $\mathcal{H}_{\text{CF}} = \Delta S^x$  and magnetic moments map onto spin-1/2 with an effective  $g$ -factor,  $g_{\text{eff}} = 2g_J \langle 0 | J_z | 1 \rangle = 13.1$ .

Similar to other rare-earth oxides with large Ising moments, we expect both nearest-neighbor (NN) exchange coupling  $J_{\text{nn}}$  and long-range dipole-dipole interactions  $D_{ij}$  in  $\text{TmMgGaO}_4$ . Given the strong quantum fluctuations in the frustrated transverse Ising model, it is non-trivial to determine the value of  $J_{\text{nn}}$  and  $\Delta$  based on the behavior of the system in zero field [26]. Instead, we apply a strong magnetic field ( $\mu_0 H$ ) along the  $c$  axis to bring  $\text{TmMgGaO}_4$  into the spin polarized state [20] and suppress quantum effects [23, 35]. Low-energy neutron-scattering measurements were conducted on the MACS spectrometer [36] at the NIST Center for Neutron Research with  $\mu_0 H = 5.5$  T and  $T = 0.1$  K. These reveal a broad and weakly dispersive spin-wave spectrum [Fig. 1(c)], which resembles that of  $\text{YbMgGaO}_4$  [23, 28]. This mode is much broader than the instrumental resolution of  $\approx 0.2$  meV and observations in zero field [19], with a full-width at half-maximum (FWHM) of 0.6 meV for the  $M$ -point excitation. Retaining the fitted peak center from fixed  $Q$  cuts, we perform fits to the spin wave excitations [black dots in Fig. 1(c)] using linear spin-wave calculations for the effective spin-1/2 Hamiltonian suitable for  $\text{TmMgGaO}_4$  [9, 19, 26]

$$\mathcal{H} = J_{\text{nn}} \sum_{\langle i,j \rangle} S_i^z S_j^z + D_{ij} \sum_{i,j} S_i^z S_j^z + \sum_i (\Delta S_i^x + h g_{\text{eff}} S_i^z), \quad (1)$$

where  $D_{ij} = D r_{\text{nn}}^3 \hat{\mathbf{z}}_i \cdot \hat{\mathbf{z}}_j - 3(\hat{\mathbf{z}}_i \cdot \hat{\mathbf{r}}_{ij})(\hat{\mathbf{z}}_j \cdot \hat{\mathbf{r}}_{ij})/r_{ij}^3$  with a strength fixed by the NN Tm-Tm distance  $r_{\text{nn}}$  and  $g_{\text{eff}}$ , and  $D = \mu_0 (g_{\text{eff}} \mu_B)^2 / (4\pi k_B r_{\text{nn}}^3) = 0.234$  meV. The best fit to the spectrum [red dashed line in Fig. 1(c)] is obtained for  $J_{\text{nn}} = 0.557(1)$  meV and  $\Delta = 0.6(1)$  meV. The value of  $\Delta$  is in reasonable agreement with previous studies [20, 26], while our obtained  $J_{\text{nn}}$  is about 20% smaller, mainly due to

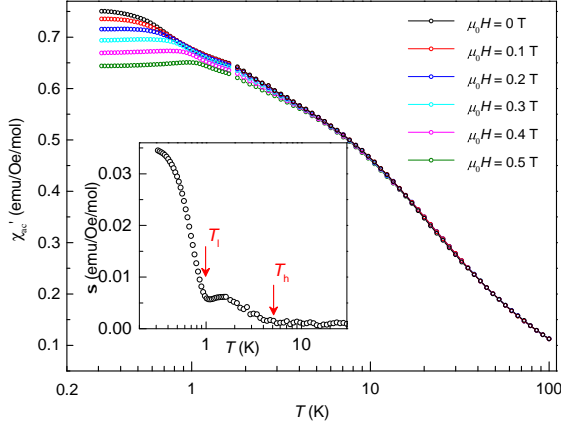


FIG. 2. Real part of the ac susceptibility ( $\chi'_{ac}$ ) measured under different dc magnetic fields  $\mu_0 H$  applied along the crystallographic  $c$ -axis and an ac field of 10 Oe with a frequency of 80 Hz. Inset: standard deviation between the six curves.

the inclusion of  $D_{ij}$  beyond the 2nd NN (see SI). We note that the broadening in both the CEF excitations and the high-field spin-wave spectra is likely due to a distribution of  $g_{\text{eff}}$  and  $\Delta$  values associated with the Mg-Ga structural disorder [20]. In this sense, the fitted values of  $\Delta$  and  $J_{\text{nn}}$  are a local-structure average.

Considering that structural disorder effects are important for the magnetization process of  $\text{TmMgGaO}_4$  [20] and that the predicted KT phase is fragile against external perturbations [24], the question naturally arises as to whether the predicted KT transitions in  $\text{TmMgGaO}_4$  survive in the zero field limit. To answer this question, we first examine the scaling behavior of the susceptibility in the proposed KT regime,  $\chi(H, T) = H^{-\alpha}$  with  $\alpha = \frac{4-18\eta(T)}{4-9\eta(T)}$  [15, 31]. Here,  $\eta(T)$  is the anomalous dimension exponent of the emergent order parameter [26], which for small  $H$  is predicted to be: (i)  $\eta(T) = 2/9$  above  $T > T_h$  so that  $\chi$  remains field-independent; (ii)  $\eta(T) \in [2/9, 1/9]$  between  $T_h$  and  $T_l$ , leading to  $H$ -dependence of  $\chi$  below  $T_h$  and divergence at  $T_l$  in the  $H \rightarrow 0$  limit; and (iii)  $\chi$  becomes flat below  $T_l$  with the onset of 3SL ordering. Our ac susceptibility measurements generally agree with these predictions. The  $\chi'_{ac}(T)$  curves begin to show noticeable  $H$ -dependence around 5 K and strongly deviate from each other below 1 K [Fig. 2 (a)]. To better illustrate this effect, we take the six data sets for  $\chi'_{ac}(T)$  corresponding to the different applied fields and compute the standard deviation at each temperature [Fig. 2 (a) inset]. Clear features are visible around 5 K and 0.9 K, which we tentatively ascribe to the two predicted transitions at  $T_h$  and  $T_l$  bounding the proposed KT phase in  $\text{TmMgGaO}_4$ . We note, however, that the ac susceptibility data deviate from theoretical predictions in certain ways. First, we do not see a divergence of  $\chi'_{ac}(T)$  at  $T_l$  as  $H \rightarrow 0$ ; instead, a peak around 0.6 K appears in the imaginary part and further moves to higher temperature with increasing  $H$  (see SI). Second, and perhaps

more significantly, we are unable to obtain a physically meaningful value of  $\eta(T)$  from the  $\chi'_{ac}(H)$  measurements at fixed temperature, since the fitted value of  $\eta(T)$  strongly depends on the choice of  $H$  (see SI). These deviations may be related to the structural disorder discussed above, where a distribution of  $g$ -factor values results in a distribution of Zeeman energies in an external magnetic field.

With evidence for two transitions seen in  $\chi'_{ac}$ , we now turn to diffuse scattering measurements performed on the CORELLI spectrometer [37] at ORNL to probe the elastic spin correlations within and below the proposed KT phase. At 0.05 K, we observe magnetic Bragg peaks at the  $K$ -points of the triangular Brillouin zone (BZ) [Fig. 3 (a)] corresponding to the 3SL order reported in previous studies [19, 20]. At 2 K (tentatively in the middle of the proposed KT phase), we see that the magnetic Bragg peaks have evolved into broad diffuse scattering with a triangular pattern, indicative of short-range 3SL correlations. These are similar to predictions from Quantum Monte-Carlo [26], although we do not observe the additional intensity predicted at the  $M$ -point within the sensitivity of our experiment.

To track the temperature dependence of the  $K$ -point intensity, we employed the HB-3A diffractometer [38] at ORNL with  $\lambda = 1.551 \text{ \AA}$ . We find that the magnetic Bragg peaks at 0.28 K display a Lorentzian shape with a FWHM of  $1.15(1)^\circ$ , which is larger than the instrumental resolution and sample mosaic of  $\Omega_G^0 = 0.53(1)^\circ$  obtained through a Gaussian fit to nuclear Bragg peaks [Fig. 3 (b)]. This points to a finite correlation length within the 2D triangular layers and no observable out-of-plane magnetic correlations (see SI). From the evolution of the  $K$ -point correlations between 0.28 and 20 K [Fig. 3 (c)], we extract the integrated peak intensity  $I$  and the intra-plane magnetic correlation length  $\xi$  according to  $\xi = \lambda / (2\Omega_L \sin \theta)$ , where  $\theta$  is the Bragg scattering angle and  $\Omega_L$  the fitted Lorentzian peak width from a Voigt function with fixed  $\Omega_G^0$ . Unlike two previous studies which reported a sharp transition at  $T_l \approx 1 \text{ K}$  based on the temperature dependence of the  $K$ -point intensity [19, 20], we see a continuous increase in both  $I$  and  $\xi$  as the temperature is lowered over a wide range [Fig. 3 (d)], with a clear exponential-dependence above 1 K. Subtle changes are observed around 0.9 K, evidenced by a flattening of  $I$  and an upturn in  $\xi$ . These observations deviate from a conventional Landau first- or second-order transition, where the local magnetic order parameter vanishes above the transition temperature [39], and provide further evidence for the continuous nature of the 3SL order and the likelihood of a KT regime. While the integrated intensity follows the exponential-law behavior up to 20 K, the signal becomes extremely broad above 3 K, limiting the range of trustworthy calculated values for  $\xi$  [Fig. 3 (c)(d)].

Further evidence of the proposed KT phase can be gained by examining the spin correlations in real space. We accomplish this through the magnetic pair distribution function (mPDF) [32, 33], which is the Fourier transform of the magnetic scattering. Our experimental mPDF data, displayed in [Fig. 4], were obtained from energy-integrated measurements



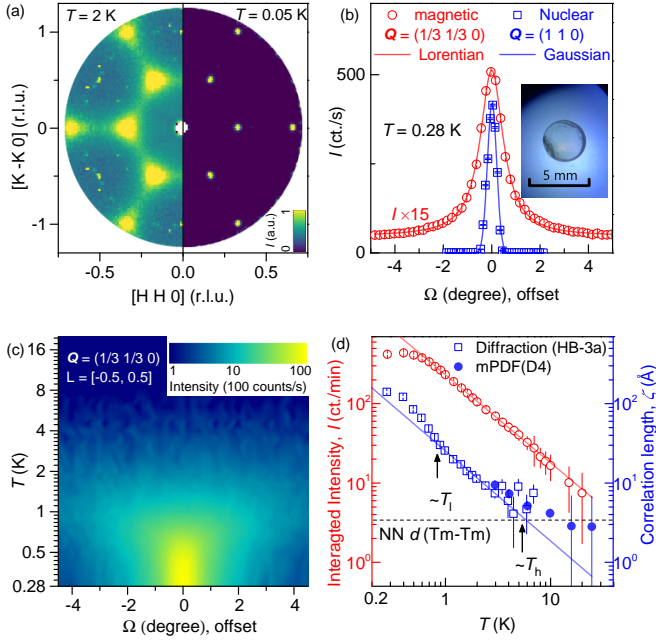


FIG. 3. (a) Magnetic diffuse scattering of the triangular-lattice Brillouin zone measured on CORELLI at  $T = 0.05$  K, 2 K, where an empty cryostat and a measurement at 40 K were used as background, respectively. Intensities were integrated within  $L = \pm 0.1$  reciprocal-lattice units (r.l.u.) and symmetrized according to the  $-3m$  point group of the Tm site. (b) Line shapes of magnetic and nuclear Bragg peaks measured on HB3A at  $T = 0.28$  K. Inset: A disk-shape single crystal sample used for the measurement. (c) Temperature dependence of the  $K$ -point magnetic Bragg peak from rocking-curve  $\Omega$ -scans. A scan at 40 K is used for background subtraction. (d) Log-log temperature dependence of the  $K$ -point peak intensity ( $I$ , red circle), and 2D correlation length ( $\xi$ , blue squares and circles) within the triangular layers. Here,  $I$  is obtained by integrating  $\Omega$  over  $[-4.5, 4.5]^\circ$ . Solid lines represent linear fit to log-log data points between 1 K and 5 K. The dashed line represents the NN Tm-Tm distance.

of a powder sample on the D4 diffractometer at the Institut Laue-Langevin [40, 41]. The negative peak at the NN distance present at all temperatures shown in Fig. 4 reflects the robust NN antiferromagnetic correlations. Additional features in the mPDF data are captured by fits [dashed black lines in Fig. 4] using the reported 3SL model with a finite correlation length  $\xi$ . The best-fit values for  $\xi$  [Fig. 3 (d)] agree well with the single-crystal diffraction analysis. The small value of  $\xi$  above  $\approx 10$  K indicates that only generic antiferromagnetic correlations between NN spins remain.

Closer inspection of the low-temperature mPDF fits [Fig. 4] reveals small but systematic misfits at the third, fourth, and fifth NN correlations. Importantly, the third NN distance shows a small, positive feature corresponding to net ferromagnetic correlations. This is at odds with the antiferromagnetic correlations predicted by the 3SL model, and may instead hint at a small component with stripe-like correlations, which have ferromagnetic alignment between third NN

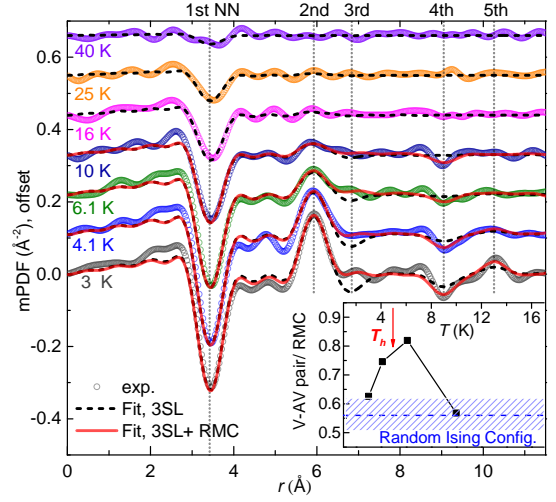


FIG. 4. Magnetic pair distribution function (mPDF) patterns (open circles) obtained at different temperatures. Dashed lines show the best fits to data using a model of the 3SL order. Solid red lines represent alternative fits combining the 3SL model with Reverse Monte Carlo (RMC) simulations of Ising spins. The  $n$ th NN in-plane Tm-Tm distances are illustrated by the vertical dotted lines. Inset: number of bounded V-AV pairs per RMC configuration as a function of temperature. For comparison, the horizontal blue dashed line shows the average number of V-AV pairs for random Ising configurations, with the shaded area representing one standard deviation.

spins [26]. To gain further insight, we performed fits combining the 3SL model with a reverse Monte Carlo (RMC) algorithm (see SI) [42]. The solid red curves in Fig. 4 show representative fits at 3, 4.1, 6.1, and 10 K, which clearly correct the mismatches left by the 3SL model.

We now look for evidence of the formation of V-AV pairs by inspecting the spin configurations produced by the RMC algorithm [see e.g. Fig. 1(d) and Supplementary Fig. 7]. 110 RMC refinements were done for each temperature, and the resulting spin configurations were analyzed to count the number of V-AV pairs. In the inset of Fig. 4, we plot the comparison of the RMC results to the expected number of V-AV pairs from randomly oriented Ising spins. The RMC refinements at 4.1 K and 6.1 K show a clear tendency for V-AV pair formation, well beyond the expectation for random spins. This is true to a lesser extent for the 3 K results, while the 10 K results fall within the underlying distribution expected for completely random spins. These findings give strong support to the formation of V-AV pairs around 4–6 K and are the strongest evidence to date for the proposed upper KT transition in  $\text{TmMgGaO}_4$ .

In summary, the magnetometry and neutron scattering results presented here establish  $\text{TmMgGaO}_4$  as a strong candidate for a solid-state system realizing KT physics. Our inelastic neutron scattering measurements confirm the transverse-field Ising model on the triangular lattice as the foundation to understand the magnetism in  $\text{TmMgGaO}_4$  and help clarify the role played by structural disorder. Magnetometry re-

veals two transitions around 0.9 K and 5 K, consistent with the theoretical predictions for a KT phase bounded by these transitions. Elastic and energy-integrated neutron scattering measurements confirm the presence of 3SL correlations in the ground state, which become gradually weaker and shorter-range as the temperature is raised. Investigation of the spin correlations in the proposed KT phase in real space via mPDF analysis suggests a tendency to form bound vortex-antivortex pairs around 5 K, which is the hallmark of the proposed KT transition. Structural disorder does not appear to play a dominant role in the zero-field physics of  $\text{TmMgGaO}_4$ , in contrast to  $\text{YbMgGaO}_4$  [23, 28–30]. Our work motivates future studies on the interplay between structural disorder effects and quantum magnetism, while also highlighting the value of mPDF analysis of short-range spin correlations in real space.

*Note Added:* In the last stages of preparation of this manuscript, we become aware of a nuclear magnetic resonance study of  $\text{TmMgGaO}_4$  [43] which finds signatures for KT transitions around 0.9 and 1.9 K.

The work of Z.L.D, M.D. and M.M. was supported by the National Science Foundation through Grant No. NSF-DMR-1750186. The work of R.B and B.F. was supported by the College of Physical and Mathematical Sciences at Brigham Young University. The work of Q.H. and H.Z. was supported by the National Science Foundation through Grant No. NSF-DMR-2003117. This research used resources at the High Flux Isotope Reactor and Spallation Neutron Source, a DOE Office of Science User Facility operated by the Oak Ridge National Laboratory. We thank the Institut Laue-Langevin for use of its neutron instrumentation. Access to MACS was provided by the Center for High Resolution Neutron Scattering, a partnership between the National Institute of Standards and Technology and the National Science Foundation under Agreement No. DMR-1508249

- 
- [1] R. B. Stinchcombe, *J. Phys. C* **6**, 2459 (1973).
  - [2] H. M. Rønnow, R. Parthasarathy, J. Jensen, G. Aeppli, T. F. Rosenbaum, and D. F. McMorrow, *Science* **308**, 389 (2005).
  - [3] S. Suzuki, J.-i. Inoue, and B. K. Chakrabarti, *Quantum Ising phases and transitions in transverse Ising models*, 2nd ed. (Springer, Heidelberg, 2012).
  - [4] R. Moessner, S. L. Sondhi, and P. Chandra, *Phys. Rev. Lett.* **84**, 4457 (2000).
  - [5] K. Kimura, S. Nakatsuji, J. Wen, C. Broholm, M. Stone, E. Nishibori, and H. Sawa, *Nat. Commun.* **4**, 1934 (2013).
  - [6] J.-J. Wen, S. M. Koohpayeh, K. A. Ross, B. A. Trump, T. M. McQueen, K. Kimura, S. Nakatsuji, Y. Qiu, D. M. Pajerowski, J. R. D. Copley, and C. L. Broholm, *Phys. Rev. Lett.* **118**, 107206 (2017).
  - [7] R. Sibille, N. Gauthier, H. Yan, M. Ciomaga Hatnean, J. Olivier, B. Winn, U. Filges, G. Balakrishnan, M. Kenzelmann, N. Shannon, and T. Fennell, *Nat. Phys.* **14**, 711 (2018).
  - [8] Z. L. Dun, J. Trinh, M. Lee, E. S. Choi, K. Li, Y. F. Hu, Y. X. Wang, N. Blanc, A. P. Ramirez, and H. D. Zhou, *Phys. Rev. B* **95**, 104439 (2017).
  - [9] Z. Dun, X. Bai, J. A. M. Paddison, E. Hollingworth, N. P. Butch, C. D. Cruz, M. B. Stone, T. Hong, F. Demmel, M. Mourigal, and H. Zhou, *Phys. Rev. X* **10**, 031069 (2020).
  - [10] Y.-L. Wang and B. R. Cooper, *Phys. Rev.* **172**, 539 (1968).
  - [11] O. Benton, *Phys. Rev. Lett.* **121**, 037203 (2018).
  - [12] L. Savary and L. Balents, *Phys. Rev. Lett.* **118**, 087203 (2017).
  - [13] J. Villain, R. Bidaux, J. P. Carton, and R. Conte, *J. Phys. Paris* **41**, 1263 (1980).
  - [14] R. Moessner and S. L. Sondhi, *Phys. Rev. B* **63**, 1 (2000), 0011250 [cond-mat].
  - [15] K. Damle, *Phys. Rev. Lett.* **115**, 1 (2015).
  - [16] J. V. José, L. P. Kadanoff, S. Kirkpatrick, and D. R. Nelson, *Phys. Rev. B* **16**, 1217 (1977).
  - [17] J. M. Kosterlitz and D. J. Thouless, *J. Phys. C Solid State Phys.*, Tech. Rep. (1973).
  - [18] F. A. Cevallos, K. Stolze, T. Kong, and R. Cava, *Materials Research Bulletin* **105**, 154 (2018).
  - [19] Y. Shen, C. Liu, Y. Qin, S. Shen, Y. D. Li, R. Bewley, A. Schneidewind, G. Chen, and J. Zhao, *Nat. Commun.* **10**, 4 (2019), 1810.05054.
  - [20] Y. Li, S. Bachus, H. Deng, W. Schmidt, H. Thoma, V. Hutanu, Y. Tokiwa, A. A. Tsirlin, and P. Gegenwart, *Phys. Rev. X* **10**, 11007 (2020), 1912.02344.
  - [21] Y. Li, G. Chen, W. Tong, L. Pi, J. Liu, Z. Yang, X. Wang, and Q. Zhang, *Phys. Rev. Lett.* **115**, 167203 (2015).
  - [22] Y. Shen, Y. D. Li, H. Wo, Y. Li, S. Shen, B. Pan, Q. Wang, H. C. Walker, P. Steffens, M. Boehm, Y. Hao, D. L. Quintero-Castro, L. W. Harriger, M. D. Frontzek, L. Hao, S. Meng, Q. Zhang, G. Chen, and J. Zhao, *Nature* **540**, 559 (2016).
  - [23] J. A. M. Paddison, M. Daum, Z. Dun, G. Ehlers, Y. Liu, M. B. Stone, H. Zhou, and M. Mourigal, *Nat. Phys.* **13**, 117 (2017).
  - [24] C. Liu, C.-J. Huang, and G. Chen, *Phys. Rev. Research* **2**, 043013 (2020).
  - [25] Z. Dun, X. Bai, M. B. Stone, H. Zhou, and M. Mourigal, arXiv:2004.10957 (2020).
  - [26] H. Li, Y. D. Liao, B. B. Chen, X. T. Zeng, X. L. Sheng, Y. Qi, Z. Y. Meng, and W. Li, *Nat. Commun.* **11**, 1 (2020), 1907.08173.
  - [27] Y.-C. Wang, Y. Qi, S. Chen, and Z. Y. Meng, *Phys. Rev. B* **96**, 115160 (2017).
  - [28] Y. Li, D. Adroja, R. I. Bewley, D. Voneshen, A. A. Tsirlin, P. Gegenwart, and Q. Zhang, *Phys. Rev. Lett.* **118**, 107202 (2017).
  - [29] Z. Zhu, P. A. Maksimov, S. R. White, and A. L. Chernyshev, *Phys. Rev. Lett.* **119**, 157201 (2017).
  - [30] I. Kimchi, A. Nahum, and T. Senthil, *Phys. Rev. X* **8**, 031028 (2018).
  - [31] S. Biswas and K. Damle, *Phys. Rev. B* **97**, 85114 (2018).
  - [32] B. A. Frandsen, X. Yang, and S. J. L. Billinge, *Acta Crystallogr. A* **70**, 3 (2014).
  - [33] B. A. Frandsen and S. J. L. Billinge, *Acta Crystallogr. A* **71**, 325 (2015).
  - [34] G. E. Granroth, A. I. Kolesnikov, T. E. Sherline, J. P. Clancy, K. A. Ross, J. P. C. Ruff, B. D. Gaulin, and S. E. Nagler, in *J. Phys.: Conf. Ser.*, Vol. 251 (IOP Publishing, 2010) p. 012058.
  - [35] K. A. Ross, L. Savary, B. D. Gaulin, and L. Balents, *Phys. Rev. X* **1**, 21002 (2011).
  - [36] J. A. Rodriguez, D. M. Adler, P. C. Brand, C. Broholm, J. C. Cook, C. Brocker, R. Hammond, Z. Huang, P. Hundertmark, J. W. Lynn, N. C. Maliszewskyj, J. Moyer, J. Orndorff, D. Pierce, T. D. Pike, G. Scharfstein, S. A. Smee, and R. Vilaseca, *Measurement Science and Technology* **19**, 034023 (2008).
  - [37] F. Ye, Y. Liu, R. Whitfield, R. Osborn, and S. Rosenkranz, *Journal of Applied Crystallography* **51**, 315 (2018).

- [38] B. C. Chakoumakos, H. Cao, F. Ye, A. D. Stoica, M. Popovici, M. Sundaram, W. Zhou, J. S. Hicks, G. W. Lynn, and R. A. Riedel, [Journal of Applied Crystallography](#) **44**, 655 (2011).
- [39] P. Toledano and J.-c. Toledano, *Landau Theory Of Phase Transitions, The: Application To Structural, Incommensurate, Magnetic And Liquid Crystal Systems*, Vol. 3 (World Scientific Publishing Company, 1987).
- [40] H. E. Fischer, [Comparison of diffraction data from a reactor source versus a spallation source for performing magnetic PDF-analysis \(a Round Robin test\)](#). Institut Laue-Langevin (ILL) (2019).
- [41] H. E. Fischer, G. J. Cuello, P. Palleau, D. Feltin, A. C. Barnes, Y. S. Badyal, and J. M. Simonson, [Appl. Phys. A](#) **74**, s160 (2002).
- [42] D. A. Keen and R. L. McGreevy, [Journal of Physics: Condensed Matter](#) **3**, 7383 (1991).
- [43] Z. Hu, Z. Ma, Y.-D. Liao, H. Li, C. Ma, Y. Cui, Y. Shangguan, Z. Huang, Y. Qi, W. Li, *et al.*, arXiv preprint arXiv:2010.06450 (2020).